Failure Analysis of Mortar Specimens with a Hexagonal Honeycomb Panel during Fatigue Load

Lucie Malíková[1,2], Jacek Katzer[3], Petr Miarka[1,2], Mohammad Sami Al Khazali[1,2], Stanislav Seitl[1,2*]

[1] Faculty of Civil Engineering, Brno University of Technology, Veveří 331/95, 602 00 Brno, Czech Republic
[2] Institute of Physics of Materials, Czech Academy of Sciences, Žižkova 513/22, 616 00 Brno, Czech Republic
[3] Faculty of Geoengineering, University of Warmia and Mazury in Olsztyn, Prawochenskiego St. 15, 10-720 Olsztyn, Poland
* Corresponding author, e-mail: seitl@ipm.cz

Abstract

It has been published in recent research studies that several mechanical properties of mortar reinforced with suitably spatial shaped plastic elements can be improved. Thus, a hexagonal geometric shape was chosen due to its high rigidity for this study. Stress distribution at a bi-material interface between a polymer part reinforcing a mortar specimen and the rest of the mortar part has been investigated to explain fatigue fracture behavior of rectangular specimens tested. A three-point-bending (3PB) test was simulated *via* a finite element method (FEM) considering several simplifications, and various heights of the polymer reinforcement were modeled to investigate its influence on stress redistribution. For comparison, a pure mortar specimen without any plastic elements was considered the reference. The numerical results obtained are discussed and compared to the experimental ones. Within the experimental campaign, bulk density, static properties and fatigue characteristics were tested, analyzed and discussed. Improvements in flexural strength were observed when the plastic panel was used as reinforcement, which agrees with other scientific works. Directions for future research were identified.

Keywords

fatigue failure, mortar reinforcement, 3D printed hexagonal honeycomb, finite element method (FEM), ABS plastic reinforcement

1 Introduction

One of the typical mechanical properties of concrete is its much higher resistance to compressive stresses than to tensile ones. The concrete's tension capability is about ten times lower than the compression one. This is the main reason why concrete members are reinforced on their tensile side to avoid failures caused by internal tensile stresses. This kind of reinforcement should prevent the structure from bending stresses, but concrete structures can also require reinforcement against shear forces, temperature and/or shrinkage cracking. Several concrete reinforcements have been developed, such as re-bar (steel or non-metallic), fiber-reinforced polymer sheet, pre-stressed cables, fiber-reinforcement, wire mesh reinforcement etc., see e.g., [1]. Also non-conventional types of reinforcement of concrete are becoming more and more popular [2].

Since the invention of reinforced concrete, the most widely used material for reinforcement has been steel in various forms. In the second half of the twentieth century, stirrups and meshes started to be replaced by steel fibers [3], but steel re-bars remain the most widely extended type of concrete reinforcement. Development of 3D printing brought new possibilities for strengthening of concrete members. At present, 3D printing is the best-known and disseminated additive manufacturing technology (see e.g., Kruth et al. [4] or Wong and Hernandez [5]). Various applications of 3D printing in civil engineering are discussed for instance in [6]. Skoratko and Katzer [6] shows spatial plastic elements as promising but so far underestimated types of concrete reinforcement. Katzer and Szatkiewicz [7] using plastic 3D printed elements as a stay-in-place formwork for beams is investigated and it is found out that mechanical behavior of such elements is similar to steel fiber reinforced concrete, ferrocement and reinforced concrete. Furthermore, it is concluded in the paper that it is possible to substitute steel reinforcement in concrete beams by 3D printed Acrylonitrile-Butadiene-Styrene (ABS) formwork. In the work of Katzer and Skoratko [8], three types of columns' shapes (most

common, rare, and impossible to be realized using traditional formworks – based on fractals) were investigated using 3D printed plastic columns formworks. Again, it was proved that it was possible to create concrete-plastic columns with satisfactory mechanical characteristics. It was also highlighted that fractal-based column's characteristic of ultimate destruction could be useful during earthquake, explosion and other emergency situations. 3D printed polymeric octet lattice structures were used as reinforcement to develop cementitious composites with enhanced ductility in Hu et al. [9]. Both experiments and numerical simulations were performed, and it was found out that the reinforced specimens had a significantly increased flexural ductility compared to plain mortar. All the works mentioned show that although the mechanical properties of plastic are low (in comparison to steel), a suitably suggested complex spatial shape of 3D printed plastics elements (such as rectangular cross-sections with and without ribs [7], a hexagonal honeycomb panel [10] and/or gyroid structures [11] are promising for concrete reinforcement. Moreover, substituting steel reinforcement with plastic in various concrete elements could help to make the construction industry more eco-friendly by utilizing recycled plastics for 3D printed reinforcements [12]. The innovative use of 3D printed plastic reinforcement in concrete offers a compelling path towards more sustainable construction. This approach presents several advantages, including:

- Enhanced performance: the unique flexural properties of 3D printed plastic make it ideal for unconventional applications where quasi-plastic behavior is required, such as structures exposed to impacts, vibrations, or seismic activity.
- Waste reduction: utilizing recycled plastic to create 3D printing filaments offers a novel solution for waste management [13, 14].
- Reduced steel consumption: partial substitution of steel reinforcement with plastic significantly reduces CO_2 emissions associated with steel production.
- Lower density: the significantly lower density of plastic compared to steel results in lighter concrete elements, potentially leading to reduced transportation costs and improved structural efficiency.
- Simplified recycling: the lower melting point of plastic compared to steel facilitates easier and more environmentally friendly recycling, potentially leading to the creation of new 3D printing filaments from recycled plastic.

However, this promising technology also presents challenges:

- Separation during demolition: the lack of established techniques for separating plastic reinforcement from concrete during demolition requires further research and development.
- Fire resistance: the lower melting point of plastic raises concerns about fire resistance, necessitating thorough investigation and potential design modifications for applications where fire safety is critical.

Despite these challenges, the potential of 3D printed plastic reinforcement to revolutionize the concrete industry is undeniable. By addressing these challenges through dedicated research and development, this innovative technology can pave the way for a more sustainable and environmentally responsible future for construction.

Failures of engineering structures are often assessed from the point of view of fatigue failure. This is a very crucial factor for the design of civil engineering materials, structural components and structures. It is necessary to ensure safety and reliability throughout the service life of a structure. This is particularly important for structures subjected to cyclic loading, as noted by Lee and Barr [15]. Cyclic stress can cause material failure before the strength limit is reached, making this type of failure particularly dangerous. Nevertheless, studies on investigations of various phenomena corresponding to fatigue of concrete structures are rather recent [16]. Many of them are devoted to analysis of the very important size effect which is typical for concrete as a quasi-brittle material [17, 18]. Also the authors' collective has been involved in investigations on various fatigue issues in concrete materials and structures, such as: evaluation of fatigue crack behavior in self-compacting concrete [19], comparison of S-N curves of concrete C50/60, High Performance Concrete and Alkali-Activated Concrete fatigue properties [20], evaluation of mechanical fracture properties of cement composite based on lunar aggregate simulant [21], proposal of a novel methodology for transition from the S-N field to Paris' law [22] and/or quantifying the effect of fiber content on the fatigue response of fine-grained cement-based composites [23]. All the referred works prove the ability of the authors to assess fatigue behavior of the novel structures suggested within this work.

Particularly, in this study, specimens made of combination of a conventional mortar and ABS plastic were investigated both experimentally and numerically. The goal

was to assess fatigue properties and stress distribution in the suggested reinforced specimens made of combination of mortar and 3D printed plastics.

2 Materials and specimen geometry

As mentioned above, specimens made of combination of a conventional mortar and ABS plastic were analyzed. Due to the fact, that spatial 3D printed elements are a quite new approach to reinforce concrete there is no full literature knowledge regarding their influence on mechanical properties of structural "concrete-plastic" elements [6, 24, 25]. In this work, 3D-printed hexagonal honeycomb panels (see Fig. 1) were used as a reinforcement for a rectangular mortar specimen. This shape was chosen because hexagonal honeycomb panel structures have high strength and stiffness compared to other types of structures, see [26, 27]. The hexagonal arrangement of the cells in the structure evenly distributes loads and stresses, resulting in higher load-carrying capacity and resistance to deformation. The plastic height and wall thickness were chosen using an orthogonal experiment design keeping in mind the size of specimens and technical abilities of harnessed 3-D printer. This type of design of an experiment was previously successfully used by some members of the research team while testing non-conventional fibre reinforced concretes [28]. Current research builds upon previous work with concrete elements reinforced by spatial 3D printed elements [7]. A triangular cross-section was chosen to maximize mechanical performance for the three-point-bending test. The design of the complex experimental campaign was focused on two key variables: the height of the reinforcing element (5, 10, 15 and 20 mm and the thickness of the hexagon wall (1, 1.33, 1.66 and 2 mm). In this paper, results obtained on selected reinforcement configurations are presented. The numerical study and fatigue experiment complement the research in [10], where flexural characteristics of a cement mortar prism specimen reinforced with hexagonal spatial elements were introduced and analyzed.

Mortar specimens were prepared from cement CEM I 42.5 N-NA, standardized CEN sand (EN 196-1:2016 [29]) characterized by a median grain diameter of 0.24 mm [30]

Fig. 1 A hexagonal honeycomb panel

and tap water. The mixture composition of the mortar is given in Table 1. From Table 1, the water-cement ratio of the mixture can be calculated as 225/450, thus $w/c = 0.5$.

ABS was chosen as a filament for 3D printing of reinforcing elements. It is a thermoplastic copolymer known for its durability, strength, and impact resistance [10, 30, 31]. It is a commonly used material in the manufacturing of various products such as automotive parts, toys, electronic housings, and household appliances. Its important advantages are that it is easy to shape, has good heat resistance, and can be easily colored and molded, making it a multipurpose material for a wide range of applications. Key advantages of ABS in comparison to other commonly used filaments are its toughness, heat resistance, superior aesthetics, minimal warping, and reliable bed adhesion. Additionally, ABS plastic is lightweight and has good chemical resistance, which further adds to its suitability for use in various industries. ABS has been proven effective as a material for creating non-conventional 3D printed reinforcement [7]. The key properties of the ABS filament provided by the producer are presented in Table 2. Methods of preparation and basic static and quasi static properties were thoroughly described in a previous publication, see [10].

The 3D printing process was meticulously designed to ensure that each hexagon wall consisted of three distinct layers. The wall thickness was varied, necessitating corresponding adjustments to the thickness of these layers. Printing was conducted using cores of two different sizes, 0.6 mm and 0.8 mm. All layers, including the external ones and the infill, were printed as solid structures to maximize strength in all directions. The printing speed averaged at 25 mm/s. This three-layered configuration of the hexagon walls is illustrated in a microscopic image presented in Fig. 2.

Linear elastic properties (Young's modulus and Poisson's ratio) for mortar and ABS were approximately 20 GPa and 0.2 and 2 GPa and 0.4, respectively.

16 rectangular $W \times B \times L$ mortar specimens ($40 \times 40 \times 160$ mm³) were prepared for each series, see Fig. 3. The size of hexagons, thickness (1.33 mm) and their spacing were constant for all 3D printed reinforcing elements, see Fig. 1. The bulk density measured for the reinforcement height

Table 1 Mixture composition for one batch

Ingredient	Mass (g)	Density (g/cm³)	Volume (cm³)
Standardized CEN sand (EN 196-1:2016 [29])	1350	2.650	509.4
Cement CEM I 42.5 N-NA	450	3.100	145.1
Tap water	225	1.000	225.0

Table 2 Key properties of the ABS filament used in this study

Property	Value
Density (kg/m^3)	1100
Melting point (°C)	+225
Heat deflection (HDT) at 0.455 MPa	86.6 ± 0.4 °C
Vicat softening temperature	93.8 ± 0.7 °C
Glass transition	100.5 °C
Diameter (mm)	2.85
Thermal decomposition (°C)	>+280
Tensile modulus (MPa)	1681.5
Tensile stress at yield (MPa)	38.1 ± 0.3
Tensile stress at break (MPa)	33.9
Elongation at yield (%)	3.5
Elongation at break (%)	4.8
Flexural strength (MPa) at 5.1% strain	70.5
Flexural strain at break	No break (>10%)
Flexural modulus (MPa)	2070.0
Charpy impact strength (at 23 °C)	14.2 ± 1.2 kJ/m^2 (Hinge)
Hardness	76 Shore D

Fig. 2 Microscopic view of three-layered 3D printed ABS hexagonal walls

Fig. 3 Photo of a specimen with dimensions of 40 × 40 × 160 mm

10 mm (H10) and basic mortar (H0) was 2091 22.59 kg/m^3 and 2133 ± 11.51 kg/m^3, respectively.

3 Fatigue experiment

The fatigue tests were carried out using the experimental set-up shown in Fig. 4. A computer-controlled servo-hydraulic testing machine under load control was used. The ratio of minimum stress to maximum stress in one cycle of loading in a fatigue test ($R = P_{max}/P_{min}$) was equal to 0.1. The controlled load frequency for the fatigue tests
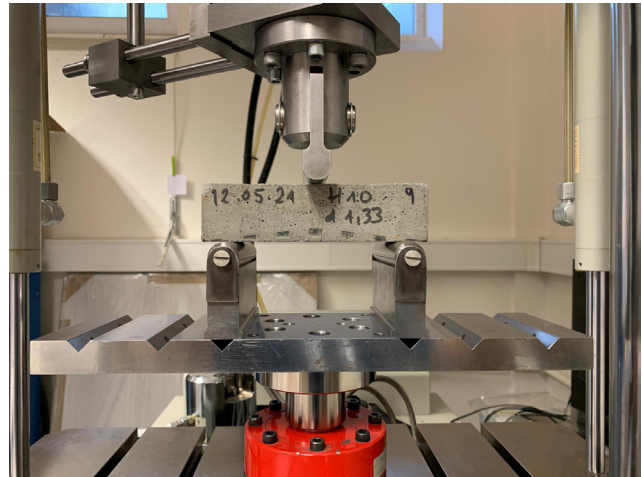
Fig. 4 Experimental set up for fatigue measurement of specimen with dimensions of 40 × 40 × 160 mm^3 (120 mm span)

was equal to 10 Hz. The fatigue endurance limit was determined based on an $S–N$ (Wöhler) curve. The number of 2×10^6 cycles was used to consider the safe applied stress amplitude (σ_a) for loading during the whole component lifetime. The experiments were performed in a laboratory with controlled temperature and humidity. The temperature was set to 23 ± 2 °C and the absolute humidity was kept at 10 g/m^3 (the corresponding relative humidity is 50 ± 2%).

Fatigue performance of materials is described by fatigue curves, which represent the dependence of fatigue lifetime on the number of cycles to failure, also known as $S–N$ (Wöhler, [32]) curves. Often, $S–N$ curves are represented as a straight line in a semi-logarithmic plot as the solution provided by Basquin's relationship [33, 34]. Accordingly, the relation between the stress range $\Delta\sigma$ and the lifetime (number of cycles N) is given by Eq. (1):

$$\Delta\sigma_a = AN^B. \tag{1}$$

where the parameters A and B represent the independent term and the slope of the resulting straight line, respectively, in double logarithmic scale.

Basquin's law is not valid in the low cycle fatigue region, so caution should be used if the calculated lifetime is low [33]. In our study, the interval of the number of cycles for the application of Basquin's relationship was from 1×10^3 up to 2×10^6 cycles (endurance limit for composites, see [35–37]).

When applying a given completely reversed stress $\Delta\sigma_a$ greater than the endurance limit, the number of stress reversals (N) after which fatigue failure will occur can be determined as:

$$N = \left(\frac{\Delta \sigma_a}{A} \right)^{\frac{1}{B}}. \tag{2}$$

4 Numerical study

Of course, the real specimen made of combination of mortar and honeycomb plastic subjected to three point bending exhibits lots of difficulties for numerical modelling. Nevertheless, to obtain basic information about the influence of the polymer reinforcement on the stress distribution in the bi-material specimen, several simplifications have been accepted (in terms of material models, geometry and boundary/interface conditions). A two-dimensional (2D) geometry of a rectangular $W \times B \times L$ (LS) mortar specimen ($40 \times 40 \times 160$ (120) mm) reinforced by a triangular polymer part of various height H subjected to three-point-bending was utilized for the parametric study. To assess the effect of the presence of the various amount of the polymer reinforcement, different heights of the polymer triangle were considered: 0; 5; 10; 15 and 20 mm. The specimen was modelled *via* finite elements (FE) in ANSYS commercial code [38]. A scheme of the specimen with boundary conditions can be seen in Fig. 5 and FE mesh with boundary conditions in Fig. 6, where also the interface is highlighted. Quadrilateral PLANE183 8-node elements were used to model the geometry of both parts of the specimen. The size of the elements varied between ca. 0.1 and 1 mm in dependence on their location, because the FE mesh was refined near the supports and the loading force. The model was made up of a total of approximately 14 thousand elements and 44 thousand nodes. Plane strain conditions were prescribed. For mortar and ABS, the linear elastic properties (Young's modulus and Poisson's ratio) were 20 GPa and 0.2 and 2 GPa and 0.4, respectively.
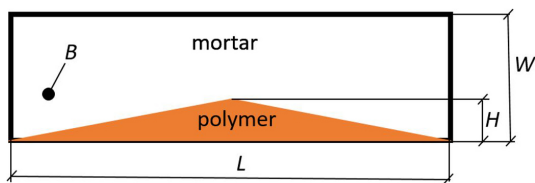

Fig. 5 Scheme of the rectangular mortar specimen ($40 \times 40 \times 160$ mm³ (120 mm span)) reinforced by an orange polymer part at its bottom subjected to three-point-bending
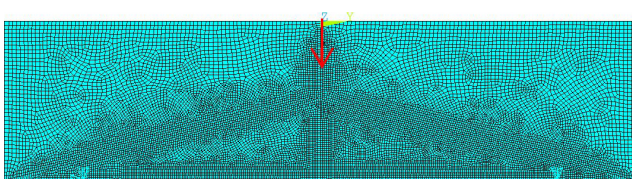

Fig. 6 FE mesh with applied boundary condition and marked interface

Thus, the linear solver was applied for solution. The interface between ABS and mortar was modelled using perfect adhesion. This assumption follows the experimental observations when the failure occurs more due to the stress concentration due to the geometry of the ABS reinforcement as no delamination between the individual materials has been observed. The stress distribution at selected places, for instance on the interface as presented in Fig. 6, was investigated for the defined force $F = 0.1$ kN and due to the linear nature of the solution it can be easily (linearly) modified to any other loading force.

5 Results and discussion

The experimentally obtained pilot fatigue results (S–N curves) for the studied composite are shown in Fig. 7, where the bending stress amplitude applied during the fatigue experiments is plotted against the logarithm of the number of cycles to failure or at 2×10^6 cycles, a limited number of cycles, for runouts, i.e., for unbroken specimens. The values of A, B describing the fatigue behavior of both configurations considered with the coefficient of determination are shown in Table 3.

Application of the hexagonal honeycomb panel increases the maximum force obtained for pure mortar specimens from static tests P_{max}(H0) = 2.21 kN (that corresponds to the stress value of 2.68 MPa) to P_{max}(H10) = 3.4 kN (that corresponds to the stress value of 4.12 MPa), but it decreases the fatigue strength of the pure mortar specimens for 2×10^6 cycles to 55% for H10, see Table 3.

Fig. 8 shows cracking patterns of ultimately destroyed specimens with H (0 and 10 mm) for different approximately given numbers of cycles, static test $N = 1$ (P_{max}), low cycle fatigue for composite $N = 1 \times 10^3$ and for high cycle regime $N = 1 \times 10^4$. It is obvious from Fig. 8 that the plain cement mortar specimens fail regularly opposite the 3PB loading and the crack propagates perpendicularly to the specimen surface, independently of the number of cycles. On the other hand, the presence of the ABS reinforcement causes stress concentrations at specific places of the bi-material specimen, which can lead to crack propagation from these locations or generally to different crack paths. Such a phenomenon could be observed in the right column of Fig. 8.

The main goal was to compare the results of the numerical simulations with experimental data obtained from both static and cyclic tests, see examples of broken specimens in Fig. 8. The tested specimens break in a specific manner in some cases and the FE simulations (see Fig. 9, where σ_1 for H10 configuration is plotted in the selected
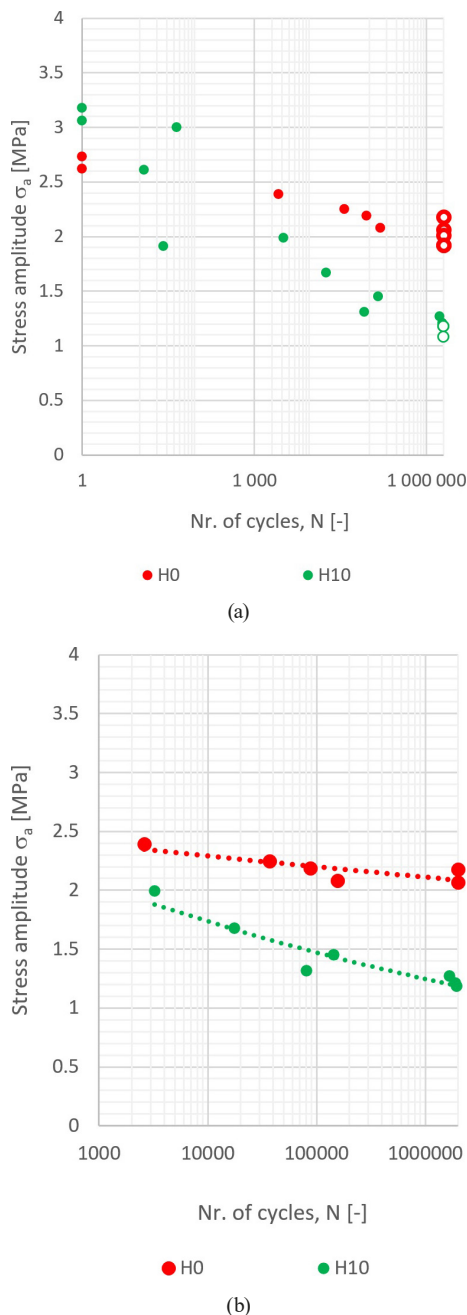
(a)

(b)

Fig. 7 Data and evaluation of H0 and H10 specimens: (a) Experimentally obtained results for H0 and H10 specimens from static test up to runout 2×10^6 (marked here by empty circles); (b) evaluation of fatigue results by Basquin's law in the interval 1×10^3 up to 2×10^6

Table 3 Values of Basquin's relationship constants A, B describing the fatigue behavior of studied specimens with and without ABS with the coefficient of determination R^2

Configuration	A	B	R^2	Fatigue strength σ_c (MPa)
H0	2.697	−0.018	0.68	2.08
H10	3.489	−0.076	0.89	1.16

range of values to better illustrate the stress distribution) should help to understand if there is some reason for such

a kind of failure. Stress tensor components as well as principal stresses were analyzed.

The stress distribution especially at the interface between the mortar and ABS element (which is probably the most important place regarding the failures observed during experiments) obtained for various reinforcement height H was compared. The interface where the stress components were investigated is highlighted in Fig. 5 and the results of the principal stress σ1 and the shear stress σ_{xy} along the interface can be found in Fig. 10.

As both plots show, the dangerous location appears both in the middle of the specimen and above the support at the polymer/mortar interface during the 3-point-bending test. The influence of the supports on the stress distribution is obvious. Of course, the exact values are affected by the size of the elements, and they include numerical errors at this specific location which is related to the way the support is modelled. Due to the set-up of the experiment, the first principal stress reaches positive values under the loading force that decrease and even change into negative values near the support, i.e., compressive stresses are presented. Shear stresses seem to be negligible along the interface, but they also exhibit a peak at the location above the support. Note that the values of the shear stress peaks in the region above the support are almost comparable to the absolute values of the principal stress. Thus, it seems that the bi-material interface above the support can be dangerous from the point of view of specimen failure. Nevertheless, as it is obvious in Fig. 8, most of the specimens fail during both static and fatigue tests in the middle of the specimen where the principal tensile stresses are the highest. The only exception is the case of mortar specimen with the plastic reinforcement loaded statically. This can be related to the above-described results of shear stresses distribution in combination with the presence of a defect at the bi-material interface near the support.

From the numerical simulations, it can be also seen that the existence of the compliant plastic reinforcement part in the mortar specimen decreases slightly the values of the principal stress along the whole interface, which could explain the higher values of critical loading forces observed experimentally during static tests. Unfortunately, fracture surface analysis on mortar materials is not so valuable as on metallic materials to be able to better understand why the fatigue strength decreases when the polymer part is presented.

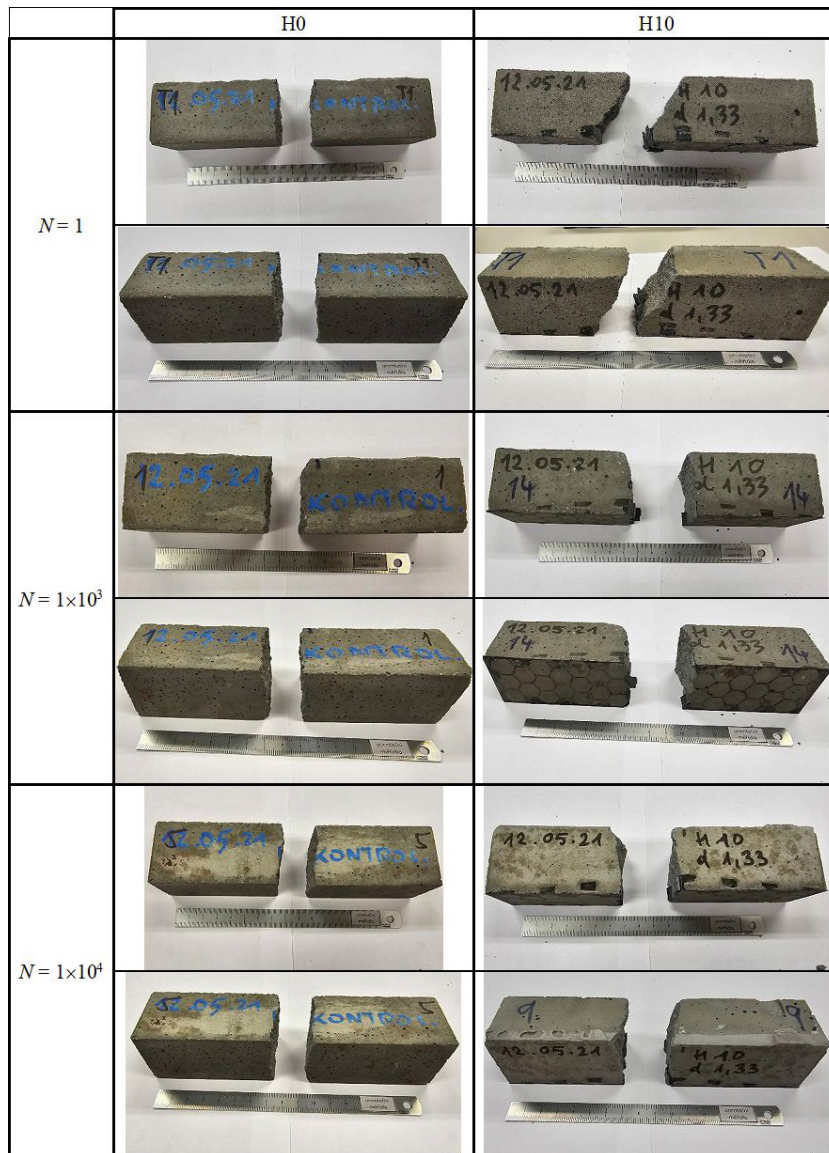Based on the results presented, the following statements can be summarized:

Fig. 8 Cracking patterns of ultimately destroyed specimens with various H (0, 10 mm) for different approx. number of cycles
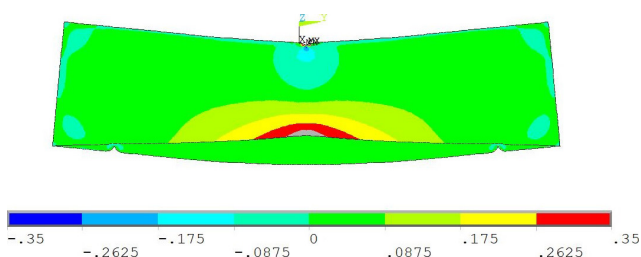

Fig. 9 Distribution of the principal stress σ_1 in MPa calculated *via* FE simulations for the H10 configuration

- Bulk density: the study indicates that bulk density is slightly decreased in the specimens made of ABS reinforced mortar. This is because ABS, which has a lower bulk density, is used in place of mortar, which has a higher bulk density. The H10 specimen exhibits a bulk density reduction of roughly 1.7% when compared to the homogenous specimen.

- Static tests: the hexagonal honeycomb panel's application increases the static characteristics. The values of P_{max}(H0) = 2.21 kN and P_{max}(H10) = 3.4 kN, correspond to the stress values of 2.68 MPa and 4.12 MPa, respectively. This can be explained by the decrease in the principal tensile stress found out numerically in specimens with compliant plastic panels.

- Fatigue properties: experimental results and *S–N* curves evaluation showed that hexagonal honeycomb panels made from ABS decrease the fatigue properties especially at the endurance limit. Thus, utilization of structures reinforced by ABS cannot be recommended for cyclically loaded structures, where fatigue failure mechanisms take place, due to different mechanisms of crack initiation. For the H10 specimens, the fatigue strength at 2×10^6 cycles is reduced to 55% compared
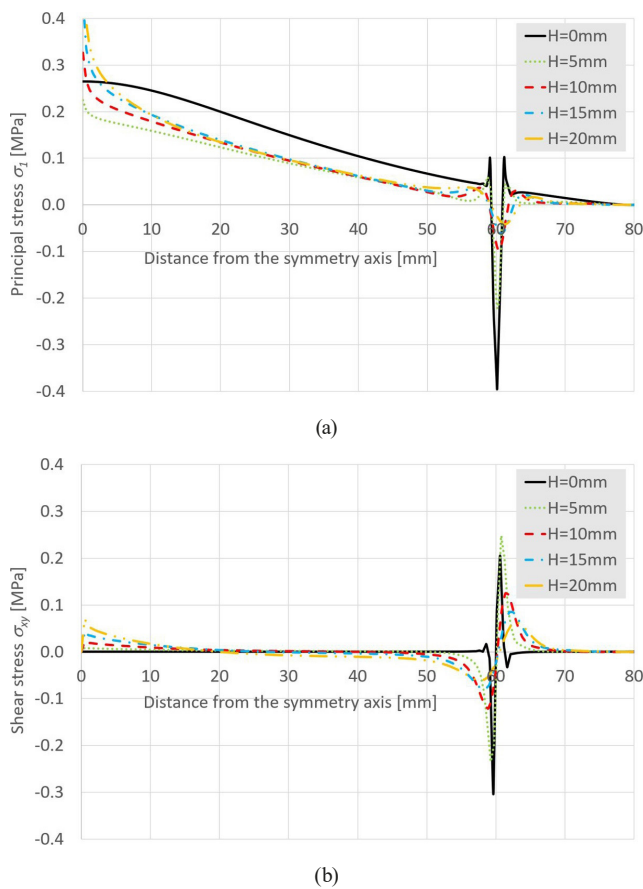
Fig. 10 Stress distribution at the bi-material interface: (a) principal stress σ_1; (b) shear stress σ_{xy}

to the H0 specimens. More both experimental (other concrete and plastic materials, other shapes of the reinforcement) and numerical (more advanced material models, boundary conditions, cohesive models) investigations can help to better understand and explain the phenomenon observed.

• Stress distribution: a numerical study *via* finite elements on a simplified numerical model of the 3PB bi-material specimen has been performed to investigate stress redistribution in a rectangular mortar specimen reinforced by a polymer part. It can be observed that dangerous locations appear both in the middle of the specimen and above the supports during the 3-point-bending test. Unfortunately, the values above the supports are distorted by numerical errors related to the way the supports are modelled. Nevertheless, the values of the shear stress peaks in this region could be comparable to the absolute values of the

principal stress. Thus, in combination with the presence of an initial defect, this place can be also dangerous from the point of view of failure. Unfortunately, an analysis of fracture surfaces on mortar materials would probably not help to better understand the mechanisms of failure. Also including the complex geometry, material models and more realistic boundary conditions into the assessment of fracture behavior of such bi-material structures is intended.

• Generally: the obtained results show that it is possible to efficiently reinforce mortar by spatial 3D printed polymer elements which is in good agreement with recent research of other scientists. The shape, size and material of a spatial 3D printed element affect the flexural behavior of a prism specimen in a wide range and this influence should be further analysed to find specific optimizations and/or general recommendations.

6 Conclusions

Selected properties of mortar specimens with a hexagonal honeycomb panel as a reinforcement was investigated. An experimental campaign was performed on both pure mortar specimens and specimens with a suggested ABS reinforcement. In addition, numerical simulations were performed to investigate stress redistribution and to support findings from the experimental campaign. It was shown that replacement of a part of the mortar specimen by a 3D printed plastic element with suitably suggested complex spatial shape can enhance the static strength of such elements which agrees with recent scientific studies. Explanation of the decrease in fatigue strength of mortar specimens containing the plastic part requires further investigations. The data used in this study can be read in [39].

References

[1] Wu, Z., Memari, A. M., Duarte, J. P. "State of the Art Review of Reinforcement Strategies and Technologies for 3D Printing of Concrete", Energies, 15(1), 360, 2022.
https://doi.org/10.3390/en15010360

[2] Harrat, O., Hadidane, Y., Anas, S. M., Sor, N. H., Deifalla, A. F., Awoyera, P. O., Gouider, N. "Nonlinear Study on the Mechanical Performance of Built-Up Cold-Formed Steel Concrete-Filled Columns Under Compression", Computer Modeling in Engineering & Sciences, 139(3), pp. 3435–3465, 2024.
https://doi.org/10.32604/cmes.2023.044950

[3] Naaman, A. E., Argon, A. S., Moavenzadeh, F. "A fracture model for fiber reinforced cementitious materials", Cement and Concrete Research, 3(4), pp. 397–411, 1973.
https://doi.org/10.1016/0008-8846(73)90078-1

[4] Kruth, J.-P., Leu, M. C., Nakagawa, T. "Progress in Additive Manufacturing and Rapid Prototyping", CIRP Annals, 47(2), pp. 525–540, 1998.
https://doi.org/10.1016/S0007-8506(07)63240-5

[5] Wong, K. V., Hernandez, A. "A Review of Additive Manufacturing", International Scholarly Research Notices, 2012(1), 208760, 2012.
https://doi.org/10.5402/2012/208760

[6] Skoratko, A., Katzer, J. "Harnessing 3D Printing of Plastics in Construction–Opportunities and Limitations", Materials, 14(16), 4547, 2021.
https://doi.org/10.3390/ma14164547

[7] Katzer, J., Szatkiewicz, T. "Properties of concrete elements with 3-D printed formworks which substitute steel reinforcement", Construction and Building Materials, 210, pp. 157–161, 2019.
https://doi.org/10.1016/j.conbuildmat.2019.03.204

[8] Katzer, J., Skoratko, A. "Concept of Using 3D Printing for Production of Concrete–Plastic Columns with Unconventional Cross Sections", Materials, 14(6), 1565, 2021.
https://doi.org/10.3390/ma14061565

[9] Hu, Y., Zhang, H., Gan, Y., Šavija, B. "Cementitious composites reinforced with 3D printed functionally graded polymeric lattice structures: Experiments and modelling", Additive Manufacturing, 39, 101887, 2021.
https://doi.org/10.1016/j.addma.2021.101887

[10] Katzer, J., Szatkiewicz, T. "Effect of 3D Printed Spatial Reinforcement on Flexural Characteristics of Conventional Mortar", Materials, 13(14), 3133, 2020.
https://doi.org/10.3390/ma13143133

[11] Skoratko, A., Szatkiewicz, T., Katzer, J., Jagoda, M. "Mechanical properties of mortar beams reinforced by gyroid 3D printed plastic spatial elements", Cement and Concrete Composites, 134, 104809, 2022.
https://doi.org/10.1016/j.cemconcomp.2022.104809

[12] Ronkay, F., Molnar, B., Gere, D., Czigany, T. "Plastic waste from marine environment: Demonstration of possible routes for recycling by different manufacturing technologies", Waste Management, 119, pp. 101–110, 2021.
https://doi.org/10.1016/j.wasman.2020.09.029

[13] Zander, N. E., Gillan, M., Lambeth, R. H. "Recycled polyethylene terephthalate as a new FFF feedstock material", Additive Manufacturing, 21, pp. 174–182, 2018.
https://doi.org/10.1016/j.addma.2018.03.007

[14] Pakkanen, J., Manfredi, D., Minetola, P., Iuliano, L. "About the Use of Recycled or Biodegradable Filaments for Sustainability of 3D Printing: State of the Art and Research Opportunities", In: Sustainable Design and Manufacturing (SDM 2017), Bologna, Italy, 2017, pp. 776–785. ISBN 978-3-319-57077-8
https://doi.org/10.1007/978-3-319-57078-5_73

[15] Lee, M. K., Barr, B. I. G. "An overview of the fatigue behavior of plain and fibre reinforced concrete", Cement and Concrete Composites, 26(4), pp. 299–305, 2004.
https://doi.org/10.1016/S0958-9465(02)00139-7

[16] Wei, X., Makhloof, D. A., Ren, X. "Analytical Models of Concrete Fatigue: A State-of-the-Art Review", CMES - Computer Modeling in Engineering and Sciences, 134(1), pp. 9–34, 2023.
https://doi.org/10.32604/cmes.2022.020160

[17] Bazant, Z. P., Xu, K. "Size Effect in Fatigue Fracture of Concrete", ACI Materials Journal, 88(4), pp. 390–399, 1991.
https://doi.org/10.14359/1786

[18] Bazant, Z. P., Schell, W. F. "Fatigue Fracture of High-Strength Concrete and Size Effect", ACI Materials Journal, 90(5), pp. 472–478, 1993.
https://doi.org/10.14359/3880

[19] Thienpont, T., De Corte, W., Seitl, S. "Self-compacting Concrete, Protecting Steel Reinforcement under Cyclic Load: Evaluation of Fatigue Crack Behavior", Procedia Engineering, 160, pp. 207–213, 2016.
https://doi.org/10.1016/j.proeng.2016.08.882

[20] Seitl, S. Miarka, P., Bílek, V. "Fatigue and fracture mechanical properties of selected concrete for subtle precast structural elements", MATEC Web of Conferences, 310, 00033, 2020.
https://doi.org/10.1051/matecconf/202031000033

[21] Seitl, S., Miarka, P., Rozsypalová, I., Pokorná, K., Keršner, Z., Katzer, J., Zarzycki, P. K. "Mechanical fracture properties of concrete with lunar aggregate simulant", MATEC Web Conferences, 323, 01014, 2020.
https://doi.org/10.1051/matecconf/202032301014

[22] Miarka, P., Seitl, S., Bílek, V., Cifuentes, H. "Assessment of fatigue resistance of concrete: S-N curves to the Paris' law curves", Construction and Building Materials, 341, 127811, 2022.
https://doi.org/10.1016/j.conbuildmat.2022.127811

[23] Domski, J., Gancarz, M., Benešová, A., Šimonová, H., Seitl, S., Frantík, P., Keršner, Z. "Effect of Tire Cords, Steel and Polypropylene Fiber Content on the Fatigue Response of Cement-Based Mortars", Advances in Science and Technology, 145, pp. 77–86, 2024.
https://doi.org/10.4028/p-5jmFQO

[24] Hack, N., Lauer, W. V. "Mesh-Mould: Robotically Fabricated Spatial Meshes as Reinforced Concrete Formwork", Architectural Design, 84(3), pp. 44–53, 2014.
https://doi.org/10.1002/ad.1753

[25] Hack, N., Lauer, W. V., Gramazio, F., Kohler, M. "Mesh Mould: Differentiation for enhanced performance", In: Proceedings of the 19th International Conference of the Association of Computer-Aided Architectural Design Research in Asia (CAADRIA 2014), Kyoto, Japan, 2014, pp. 1–10. ISBN 9881902657 [online] Available at: https://www.researchgate.net/publication/281966796_Mesh-Mould_Differentiation_for_Enhanced_Performance#fullTextFileContent [Accessed: 14 November 2024]

[26] Habib, F. N., Iovenitti, P., Masood, S. H., Nikzad, M. "Cell geometry effect on in-plane energy absorption of periodic honeycomb structures", The International Journal of Advanced Manufacturing Technology, 94(5), pp. 2369–2380, 2018.
https://doi.org/10.1007/s00170-017-1037-z

[27] Goldmann, T., Huang, W.-C., Rzepa, S., Džugan, J., Sedláček, R., Daniel, M. "Additive Manufacturing of Honeycomb Lattice Structure—From Theoretical Models to Polymer and Metal Products", Materials, 15(5), 1838, 2022.
https://doi.org/10.3390/ma15051838

[28] Katzer, J., Domski, J. "Optimization of fibre reinforcement for waste aggregate cement composite", Construction and Building Materials, 38, pp. 790–795, 2013.
https://doi.org/10.1016/j.conbuildmat.2012.09.057

[29] CEN "EN 196-1:2016 Methods of testing cement – Part 1: Determination of strength", European Committee for Standardization, Brussels, Belgium, 2016.

[30] Katzer, J. "Median diameter as a grading characteristic for fine aggregate cement composite designing", Construction and Building Materials, 35, pp. 884–887, 2012.
https://doi.org/10.1016/j.conbuildmat.2012.04.050

[31] Tymrak, B. M., Kreiger, M., Pearce, J. M. "Mechanical properties of components fabricated with open-source 3-D printers under realistic environmental conditions", Materials & Design, 58, pp. 242–246, 2014.
https://doi.org/10.1016/j.matdes.2014.02.038

[32] Wöhler, A. "Versuche uber die Festigkeit der Eisenbahnwagenachsen" (Experiments on the strength of metals), Zeitschrift für Bauwesen, 10(4), pp. 160–161, 1867. (in German)

[33] Basquin, O. H. "The Exponential Law of Endurance Tests", American Society for Testing and Materials Proceedings, 10, pp. 625–630, 1910.

[34] Seitl, S., Miarka, P., Šimonová, H., Frantík, P., Keršner, Z., Domski, J., Katzer, J. "Change of Fatigue and Mechanical Fracture Properties of a Cement Composite due to Partial Replacement of Aggregate by Red Ceramic Waste", Periodica Polytechnica Civil Engineering, 63(1), pp. 152–159, 2019.
https://doi.org/10.3311/PPci.12450

[35] Ramakrishnan, V., Wu, G. Y., Hosalli, G. "Flexural Fatigue Strength, Endurance Limit, and Impact Strengths of Fiber Reinforced Concrete", Transportation Research Record, 1226, pp. 17–24, 1989. [online] Available at: http://onlinepubs.trb.org/Onlinepubs/trr/1989/1226/1226-003.pdf [Accessed: 14 November 2024]

[36] Sobhan, K., Das, B. M. "Durability of Soil–Cements against Fatigue Fracture", Journal of Materials in Civil Engineering, 19(1), pp. 26–32, 2007.
https://doi.org/10.1061/(ASCE)0899-1561(2007)19:1(26)

[37] Beriha, B., Sahoo, U. C., Steyn, W. J. "Determination of endurance limit for different bound materials used in pavements: A review", International Journal of Transportation Science and Technology, 8(3), pp. 263–279, 2019.
https://doi.org/10.1016/j.ijtst.2019.05.002

[38] ANSYS "Finite element software, (2021 R2)", [computer program] Available at: https://www.ansys.com/ [Accessed: 14 November 2024]

[39] Malikova, L., Katzer, J., Miarka, P., Al Khazali, M. S., Seitl, S. "Failure analysis of mortar specimens with a hexagonal honeycomb panel during fatigue load", [preprint] Zenodo, 09 October 2024.
https://doi.org/10.5281/zenodo.13906216